

Thermochemistry of solvation: A self-consistent three-dimensional reference interaction site model approach

Andriy Kovalenko^{a)} and Thanh N. Truong^{b)}

Henry Eyring Center for Theoretical Chemistry, Department of Chemistry, University of Utah, 315 S 1400 E, rm 2020, Salt Lake City, Utah 84112-0850

(Received 11 April 2000; accepted 4 August 2000)

We developed a self-consistent three-dimensional reference interaction site model integral equation theory with the molecular hypernetted chain closure (SC-3D-RISM/HNC) for studying thermochemistry of solvation of ionic solutes in a polar molecular solvent. It is free from the inconsistency in the positions of the ion-solvent site distribution peaks, peculiar to the conventional RISM/HNC approach and improves the predictions for the solvation thermodynamics. The SC-3D-RISM treatment can be readily generalized to the case of finite ionic concentrations, including the consistent dielectric corrections to provide a consistent description of the dielectric properties of ion-molecular solution. The proposed theory is tested for hydration of the Na^+ and Cl^- ions in ambient water at infinite dilution. An improved agreement of the ion hydration structure and thermodynamics with molecular simulation results is found as compared to the conventional RISM/HNC treatment. © 2000 American Institute of Physics. [S0021-9606(00)51941-2]

I. INTRODUCTION

Understanding and prediction of solvation properties of electrolytes is of paramount importance for solution chemistry as well as for biological systems. The presence of ions in aqueous solution has an essential effect on conformational stability and binding of proteins and DNA.¹⁻³ Ionic effects play a central role at all levels of DNA structural organization.^{4,5} Molecular simulations can reliably model solvation of small molecules, whereas the solvation thermodynamics of biomolecules in electrolyte solution constitutes a considerable challenge for simulation because of their big size as well as long-range ionic correlations in solution at typically intermediate and low salt concentrations. Alternatively, these problems can be resolved within integral equation theory of liquids. An integral equation theory providing realistic description for molecular liquids is the reference interaction site model (RISM).⁶ It was pioneered by Chandler and Andersen⁷ and then extended by Hirata and co-workers to dipolar and quadrupolar molecular liquids^{8,9} and to ions in a polar molecular solvent¹⁰ by adapting the hypernetted chain (HNC) closure. As an advantage over other integral equation theories for molecular liquids,⁶ the RISM can easily handle the description of solution comprising complex polyatomic species and to take into account such chemical specificities as hydrogen bonding.¹¹ Pettitt and Rossky¹² employed the extended RISM approach to qualitatively predict liquid state structure for three-site models of water. The RISM integral equation theory has been successfully used in calculation of the structural and thermodynamic properties of various chemical and biological systems and solutions.¹¹

Along with its merits, the RISM/HNC approach suffers from a number of defects. It is known to yield essentially trivial results for the dielectric constant of a polar molecular liquid,^{8-10,13,14} and to fail at finite salt concentrations due to an inherent dielectric inconsistency.^{15,16} Perkyns and Pettitt¹⁵ have obviated this problem by introducing consistent corrections that are similar to a bridge function of molecular theories. The dielectrically consistent DRISM/HNC approach yields accurate thermodynamics and structure in 1-1 salt aqueous solutions at finite concentrations.¹⁵

Another shortcoming of the RISM/HNC theory lies in the imperfect treatment of excluded volume of interaction sites constituting the molecular species. It results, for instance, in substantial overestimation of the excess chemical potential of hydrophobic hydration and its wrong dependence on the hydrophobic solute size.^{19,20} This mistreatment can be corrected by employing closures other than the HNC approximation²¹ or by introducing bridge corrections of various parameterized form.^{23,24} A well-documented manifestation of the excluded volume inconsistency is related to the problem of so-called auxiliary sites that label points in a molecule but contribute nothing to the intermolecular potential.^{6,17,18} It also shows up in the site-site radial distributions between strongly attracting interaction sites situated inside molecular cores, which are predicted to approach each other closer than is allowed by the steric constraints of the molecular shapes. Although the RISM integral equation accounts for the intramolecular bond constraints by means of the intramolecular matrix, its HNC closure treats the interaction sites of molecules as free, nonbonded species. As an example, the RISM/HNC approach yields the separation between the peaks of water oxygen and hydrogen interaction sites around an anion in aqueous solution to be somewhat larger than the OH intramolecular bond length in a water molecule.^{16,22,25}

^{a)}Present address: Institute for Molecular Science, Myodaiji, Okazaki, Aichi 444-8585, Japan.

^{b)}Author to whom correspondence should be addressed. Electronic mail: truong@mercury.hec.utah.edu

An alternative way to consider molecular systems is to use the Ornstein–Zernike (OZ) integral equation generalized to the six-dimensional (6D) case of orientationally dependent interactions, or the molecular Ornstein–Zernike (MOZ) equation,⁶ and then to employ Blum’s method of rotationally invariant expansions in the generalized spherical harmonics.²⁶ The MOZ methodology was successfully applied to models of real molecular fluids²⁷ and organic solvents.²⁸ Recently, this treatment has been employed by Richardi, Millot, and Fries²⁹ for different models of water and methanol, and by Lombardero and co-workers³⁰ to describe the simple point charge (SPC) water in a variety of thermodynamic states. By using the method of rotational invariant expansions, Beglov and Roux³¹ formulated the three-dimensional (3D) generalization of the OZ equation with the mean spherical approximation (MSA) closure for the distribution of a liquid of spherical molecules with an embedded dipole around a polar solute of arbitrary form. Richardi, Fries, and Krienke³² developed the MOZ/HNC description of solvation of spherical ions in acetonitrile and acetone. In the above works, the MOZ integral equation approach provides a detailed, complete information about the solvation structure, and the solvation thermodynamics in good qualitative agreement with molecular simulations. As an advantage, it does not share the above-mentioned problems of the RISM integral equation theory with excluded volume. However, such a treatment quickly becomes increasingly cumbersome with asphericity of solvent molecules because of the slow convergence of rotational invariant expansions, especially in the general case of solvent molecules not possessing any rotational symmetry like acetonitrile or acetone in Ref. 32. This justifies further efforts in improvement of the RISM theory and, in particular, development of its 3D version.

A much more detailed solvation structure information can be obtained from the 3D generalization of the RISM theory which yields 3D distribution profiles of solvent interaction sites around a solute of arbitrary shape. It was first derived by Chandler, McCoy, and Singer in a general form within the density functional method for nonuniform polyatomic systems,³³ and recently developed by Cortis, Rosky, and Friesner for a one-component dipolar molecular liquid,³⁴ by Beglov and Roux for water and organic molecules in water,^{23,35} and by Kovalenko and Hirata for water,^{36,37} metal–water interfaces,^{36,39} 3D potentials of mean force for molecular ions in a polar organic solvent,³⁸ and ion pairs in water.⁴⁰ A self-consistent 3D-RISM description of a one-component molecular liquid is obtained by considering one molecule as a “solute” immersed in solvent of other molecules of liquid to calculate the 3D “solvent–solvent” correlations, and then averaging them for the solute orientations to get the site–site solvent–solvent correlation functions used as input to the 3D-RISM solute–solvent equations.^{34,37} The 3D-RISM approach allows one to calculate the potentials of mean force in ion-molecular solution directly as a difference between the chemical potential of solvation of a cluster of solutes and of individual ones, and to obtain the solvation structure around the cluster of solutes in detail.⁴⁰ It should be noted that accurate calculation of solvation thermodynamics for ionic solutes in a polar molecular liquid

requires special corrections for a finite size of the supercell which is employed within the 3D-RISM method.⁴⁰

A considerable advantage of the 3D-RISM theory is proper description of the excluded volume of a solute, owing to the explicit account of its 3D shape. By formulating a self-consistent 3D-RISM approach for ions in a polar molecular liquid, this allows us to eliminate the above-mentioned problem with violation of steric constraints in the ion–solvent site distributions. In this procedure, we obtain the 3D potential of mean force between the ion and one molecule of liquid, each considered as solutes immersed in solvent of liquid. Radial distribution functions between the ion and the interaction sites of solvent molecules are required at input, which are calculated in a self-consistent loop by orientational averaging of the 3D distribution of the ion around the labeled molecule of liquid. The whole approach can be readily generalized to the case of a finite ionic concentration; this will be considered in further work. The self-consistent 3D-RISM theory (SC-3D-RISM) we propose below improves the description of the solvation structure and thermodynamics of simple ions in a polar molecular liquid as compared to the conventional, one-dimensional (1D) RISM method. Section II presents the SC-3D-RISM/HNC equations for an ion at infinite dilution. Section III gives a derivation of the expressions for the excess chemical potential, energy, entropy, and enthalpy of solvation. Section IV introduces corrections necessary for proper account of the effect of the long-range asymptotics of the correlation functions on the solvation thermodynamics. Section V illustrates the approach by calculation of the solvation structure and thermodynamics for Na⁺ and Cl[−] ions in ambient water.

II. SELF-CONSISTENT 3D-RISM THEORY FOR A SIMPLE ION IN A POLAR MOLECULAR LIQUID

The orientation-dependent distribution function between two molecular species immersed in a molecular solvent can be obtained from the 3D-RISM equations for a solute-solvent mixture at infinite dilution.³⁸ In this procedure, the solvent contribution to the orientationally dependent potential of mean force between two molecular solutes through interaction sites of solvent molecules is calculated as a convolution of the 3D site correlation functions of solvent molecular sites around each of the solutes. The solute–solute distribution thus has full six-dimensional orientational dependence, whereas solvent molecules are described at the interaction site level with their orientations averaged out. For a simple ion immersed in a polar molecular liquid, the problem simplifies to a 3D distribution of the ion around one solute molecule of liquid, both immersed in the solvent of liquid. The MOZ equation for the solvent–ion correlations at infinite dilution is written as⁶

$$h^{si}(r, \Omega) = c^{si}(r, \Omega) + \frac{\rho}{\Omega} \int \mathbf{dr}' d\Omega' c^{ss} \times (|\mathbf{r} - \mathbf{r}'|, \Omega, \Omega') h^{si}(r', \Omega'), \quad (1)$$

where the superscripts “*i*” and “*s*” denote the ion and solvent; *h* and *c* are, respectively, the total correlation function (TCF) and the direct correlation function (DCF) that depend

on the separation r between the corresponding species and on orientation Ω of solvent molecules; ρ is the solvent density. We need to reduce in part the orientational dependence of the 6D argument of $c^{ss}(r, \Omega, \Omega')$ by integrating out the orientational degrees of freedom in (1). Notice that due to the isotropy of the bulk system under consideration, one orientational degree of freedom of the Euler angles Ω and Ω' is dependent. That is, the 6D argument comprises the distance r and *five* independent angles in Ω, Ω' . In what follows, we fix the third angle ψ in the orientation $\Omega = (\varphi, \theta, \psi)$, which brings the 6D argument into the form of a vector between the particles and the 3D orientation of the second particle, $(r, \Omega, \Omega') = (r, \varphi, \theta, \Omega') \equiv (\mathbf{r}, \Omega')$. Similarly to Refs. 34, 38, and 39, we assume the decomposition of the DCF into partial contributions of sites of a solvent molecule

$$c^{ss}(r, \Omega, \Omega') \equiv c^{ss}(\mathbf{r}, \Omega') = \sum_{\alpha} c_{\alpha}^{ss}(\mathbf{r} + \mathbf{r}_{s\alpha}), \quad (2)$$

where $\mathbf{r}_{s\alpha}$ is the shift of interaction site α of the solvent molecule with respect to its origin. Here the partial, 3D site DCFs $c_{\alpha}^{ss}(\mathbf{r})$ do not depend on the solvent molecule orientation, Ω' , since each its site is considered to be spherically symmetric. This basic assumption of additivity in the 3D-RISM theory is justified since the DCF has the long-range asymptotics of the interaction potential which is supposed to be additive, $c^{ss}(\mathbf{r}, \Omega') \sim -\beta \sum_{\alpha} u_{\alpha}^{ss}(\mathbf{r}_{\alpha})$ for $r \rightarrow \infty$, where $\beta = 1/k_B T$ is the inverse temperature, and \mathbf{r}_{α} is the position of interaction site α of solvent molecule 2 with respect to solvent molecule 1. On transformation to the reciprocal space, the decomposition (2) takes the form

$$c^{ss}(\mathbf{k}, \Omega') = \sum_{\alpha} c_{\alpha}^{ss}(\mathbf{k}) \exp(-i\mathbf{k} \cdot \mathbf{r}_{s\alpha}), \quad (3)$$

in which the dependence on solvent orientation Ω' goes into the phase factor $\exp(-i\mathbf{k} \cdot \mathbf{r}_{s\alpha})$. In the reciprocal space, the convolution in the MOZ equation (1) turns into multiplication, and substitution of relation (3) allows one to carry out the integration over the orientation Ω' . This reduces the 3D solvent-ion TCF to the radial one between the ion and solvent site α , according to the definition of the orientational average

$$h_{\alpha}^{si}(r) = \frac{1}{\Omega} \int d\Omega_{\mathbf{r}} h^{si}(\mathbf{r}_{s\alpha} + \mathbf{r}), \quad (4a)$$

$$h_{\alpha}^{si}(k) = \frac{1}{\Omega} \int d\Omega_{\mathbf{k}} h^{si}(\mathbf{k}) \exp(-i\mathbf{k} \cdot \mathbf{r}_{s\alpha}). \quad (4b)$$

Thus, we obtain the 3D-RISM equation for the 3D correlations $h^{si}(\mathbf{r})$ and $c^{si}(\mathbf{r})$ of the ion around the solvent molecule

$$h^{si}(\mathbf{r}) = c^{si}(\mathbf{r}) + \rho \sum_{\alpha} c_{\alpha}^{ss}(\mathbf{r}) * h_{\alpha}^{si}(r), \quad (5)$$

where $h_{\alpha}^{si}(r)$ is the radial TCF between the ion and solvent site α , $c_{\alpha}^{ss}(\mathbf{r})$ is the 3D-DCF of solvent site α around a labeled molecule in pure molecular solvent, and “*” means convolution in direct space. The 3D site correlation functions are specified on a uniform 3D grid in a rectangular supercell,

and the convolution in (5) is calculated by transformation to reciprocal space with the 3D fast Fourier transform (3D-FFT).⁴¹

To treat the problem self-consistently, the ion-solvent site radial TCFs $h_{\alpha}^{si}(r)$ are calculated numerically by the orientational averaging using Eqs. (4). As proposed in Ref. 37, we apply the averaging to the Fourier expansion of $h^{si}(\mathbf{r})$. It simply reduces the expansion in 3D plane waves to that in spherical ones

$$\begin{aligned} h_{\alpha}^{si}(r) &= \frac{1}{\Omega} \int d\Omega_{\mathbf{r}} \sum_{\mathbf{k}} h^{si}(\mathbf{k}) \exp(-i\mathbf{k} \cdot \mathbf{r}_{s\alpha}) \\ &= \sum_{\mathbf{k}} \frac{\sin(kr)}{kr} \sum_{|\mathbf{k}|=k} \exp(-i\mathbf{k} \cdot \mathbf{r}_{s\alpha}) h^{si}(\mathbf{k}), \end{aligned} \quad (6)$$

with the phase factor $\exp(-i\mathbf{k} \cdot \mathbf{r}_{s\alpha})$ arising due to the shift of the averaging center from the origin to site α . The orientational averaging procedure thus consists in performing the 3D-FFT, summing the expansion coefficients with equal absolute values of wave vector \mathbf{k} , and then synthesizing $h_{\alpha}^{si}(r)$ of spherical waves on a linear one-dimensional (1D) radial grid. Finally, the radial distribution functions are transformed by the linear 1D-FFT, and then splined to obtain $h_{\alpha}^{si}(k)$ at wave vector absolute values k necessary for the 3D convolution in (5). The parameters of the 1D grid are chosen in such a way as to override the resolution of the 3D grid in real and reciprocal spaces. The functions $h_{\alpha}^{si}(r)$ are calculated by Eq. (6) inside a sphere, $r < L_{\max}/2$, where L_{\max} is the largest dimension of the supercell, $L_{\max} = \max(L_x, L_y, L_z)$, and are padded with zeros outside it. The above procedure of orientational averaging is substantially faster than quadrature schemes, for example, Lebedev's quadrature method employed by Cortis, Rossky, and Friesner.³⁴ As we have discussed in Ref. 37, the approach given by Eq. (6) distorts the averaged radial correlation function by an artifact of small oscillations with the frequency equal to the cutoff of the plane wave set used. However, this is of no importance since such oscillations are smoothed out in the convolution procedure in (5), and introduces a negligible error.

To close the solvent-ion 3D-RISM equation (5), we use the HNC approximation which is proved to be adequate for ion-molecular systems with long-range electrostatic interactions.⁶ The molecular 3D-HNC closure is written as

$$g^{si}(\mathbf{r}) = \exp(-\beta u^{si}(\mathbf{r}) + h^{si}(\mathbf{r}) - c^{si}(\mathbf{r})), \quad (7)$$

where $u^{si}(\mathbf{r})$ is the 3D interaction potential between the ion and the molecule of liquid, and $g^{si}(\mathbf{r}) = h^{si}(\mathbf{r}) + 1$ is the 3D distribution function of the ion around the molecule. With this closure, the solvent-ion 3D-RISM/HNC equations to be solved can be cast in the form

$$h^{si}(\mathbf{r}) + 1 = \exp\left(-\beta u^{si}(\mathbf{r}) + \rho \sum_{\alpha} c_{\alpha}^{ss}(\mathbf{r}) * h_{\alpha}^{si}(r)\right), \quad (8)$$

where h_{α}^{si} are calculated by using Eq. (6). Notice that unlike the 3D-HNC approximations for the 3D correlations of solvent interaction sites around the solute,³⁴⁻⁴⁰ the molecular 3D-HNC closure (7) relates the 3D correlations between the ion and the *entire* solvent molecule. This provides consis-

tency of the solvent–ion correlations, in particular, ensures the steric constraints for the ion–solvent site distributions.

We determine the 3D site DCFs of pure solvent around its labeled molecule, $c_{\alpha}^{ss}(\mathbf{r})$, from the SC-3D-RISM/HNC equations for a one-component molecular liquid³⁷

$$h_{\gamma}^{ss}(\mathbf{k}) = \sum_{\alpha} c_{\alpha}^{ss}(\mathbf{k}) (\omega_{\alpha\gamma}^{ss}(k) + \rho h_{\alpha\gamma}^{ss}(k)), \quad (9)$$

$$g_{\alpha}^{ss}(\mathbf{r}) = h_{\alpha}^{ss}(\mathbf{r}) + 1 = \exp(-\beta u_{\alpha}^{ss}(\mathbf{r}) + h_{\alpha}^{ss}(\mathbf{r}) - c_{\alpha}^{ss}(\mathbf{r})), \quad (10)$$

where the radial TCF between sites α and γ of two molecules in pure solvent, $h_{\alpha\gamma}^{ss}(r)$, are calculated by the orientational averaging

$$\begin{aligned} h_{\alpha\gamma}^{ss}(r) &= \frac{1}{\Omega} \int d\Omega_{\mathbf{r}} h_{\gamma}^{ss}(\mathbf{r}_{s\alpha} + \mathbf{r}) \\ &= \sum_{\mathbf{k}} \frac{\sin(kr)}{kr} \sum_{|\mathbf{k}|=k} \exp(-i\mathbf{k} \cdot \mathbf{r}_{s\alpha}) h_{\gamma}^{ss}(\mathbf{k}). \end{aligned} \quad (11)$$

Here $u_{\alpha}^{ss}(\mathbf{r})$ is the interaction potential between solvent site α and the labeled solvent molecule, and $\omega_{\alpha\gamma}^{ss}(r) = \delta(r - l_{\alpha\gamma})$ is the intramolecular correlation matrix of a solvent molecule with site–site separations $l_{\alpha\gamma}$, or in reciprocal space $\omega_{\alpha\gamma}^{ss}(k) = \sin(kl_{\alpha\gamma})/(kl_{\alpha\gamma})$. Although Eqs. (9)–(11) provide a consistent description of the labeled molecule of the solvent, they do not resolve the problem of auxiliary sites for the solvent–solvent correlations. However, this is not crucial since such an artifact manifests in the correlations between polar molecules much less than in those between ions and polar molecules. Further improvement would require either treatment of 6D solvent–solvent correlations or inclusion of bridge corrections in the 3D-HNC closure for the 3D site correlations (10). Such an improvement will be addressed elsewhere.

An alternative formulation of the solvent-ion 3D-RISM equation can be obtained by the orientational reduction of the MOZ equation (1) with the term representing interaction over the “third particle” written as $\int d\mathbf{3}h^{ss}(13)c^{si}(32)$. It has the form

$$h^{si}(\mathbf{k}) = c^{si}(\mathbf{k}) + \rho \sum_{\alpha} h_{\alpha}^{ss}(\mathbf{k}) c_{\alpha}^{si}(k), \quad (12)$$

with the ion-solvent site radial DCF $c_{\alpha}^{si}(r)$ obtained self-consistently from the approximate decomposition of the 3D-DCF $c^{si}(\mathbf{r})$ into partial site contributions similarly to (2)

$$c^{si}(\mathbf{r}) = \sum_{\alpha} c_{\alpha}^{si}(|\mathbf{r} - \mathbf{r}_{s\alpha}|). \quad (13)$$

The latter can be performed by orientationally averaging the 3D-DCF

$$\bar{c}_{\alpha}^{si}(r) = \frac{1}{\Omega} \int d\Omega_{\mathbf{r}} c^{si}(\mathbf{r}_{s\alpha} + \mathbf{r}), \quad (14)$$

and then decomposing the *averaged* ion–solvent site radial DCFs \bar{c}_{α}^{si} into the *partial* site contributions c_{α}^{si} by using the relation following from the assumption of Eq. (13)^{34,38,39}

$$\bar{c}_{\alpha}^{si}(k) = \sum_{\gamma} \omega_{\alpha\gamma}^{ss}(k) c_{\gamma}^{si}(k). \quad (15)$$

In a similar manner, the 3D site DCFs of pure solvent can be determined alternatively from the method proposed by Cortis, Rossky, and Friesner³⁴ by the molecular site Ornstein–Zernike integral equation with the HNC approximation (MSOZ/HNC), which can be written as

$$h_{\gamma}^{ss}(\mathbf{k}) = \sum_{\alpha} (c_{\alpha}^{ss}(\mathbf{k}) \omega_{\alpha\gamma}^{ss}(k) + \rho h_{\alpha}^{ss}(\mathbf{k}) c_{\alpha\gamma}^{ss}(k)), \quad (16)$$

$$g_{\alpha}^{ss}(\mathbf{r}) = h_{\alpha}^{ss}(\mathbf{r}) + 1 = \exp(-\beta u_{\alpha}^{ss}(\mathbf{r}) + h_{\alpha}^{ss}(\mathbf{r}) - c_{\alpha}^{ss}(\mathbf{r})), \quad (17)$$

with the orientational averaging of the solvent 3D site DCFs $c_{\alpha}^{ss}(\mathbf{r})$ and then the decomposition of the *averaged* site–site DCFs $\bar{c}_{\alpha\gamma}^{ss}(r)$ into the radial site–site DCFs $c_{\mu\gamma}^{ss}(r)$

$$\bar{c}_{\alpha\gamma}^{ss}(r) = \frac{1}{\Omega} \int d\Omega_{\mathbf{r}} c_{\gamma}^{ss}(\mathbf{r}_{s\alpha} + \mathbf{r}), \quad (18)$$

$$\bar{c}_{\alpha\gamma}^{ss}(k) = \sum_{\mu} \omega_{\alpha\mu}^{ss}(k) c_{\mu\gamma}^{ss}(k). \quad (19)$$

It should be emphasized that the solvent–ion SC-3D-RISM equations in the formulation (12) with the 3D-DCF averaging and decomposition relations (14) and (15) are *not* equivalent to Eq. (5) with the 3D-TCF orientational averaging given by Eq. (4). The additive approximation in Eq. (13) or (15) is exact only in the long-range asymptotic limit and thus decreases the level of accuracy of the solvent–ion correlations. Furthermore, calculation of the ion–solvent site radial DCF c_{α}^{si} from relation (15) involves the inverse of the intramolecular matrix, which has a singularity at $k=0$. Due to the electroneutrality condition, the singularity is cancelled out in the summation over interaction sites γ , which requires special evaluation of the averaged $\bar{c}_{\alpha}^{si}(k=0)$ and introduces additional numerical errors. In the case when the approximation (13) becomes too crude, the decomposition procedure can cause instability and even divergence.

Similar properties distinguish the solvent–solvent SC-3D-RISM/HNC equations (9)–(11) from the MSOZ equations (16)–(19) of Cortis, Rossky, and Friesner.³⁴ The former *do not* involve the additive approximation (19), and employ simply the orientational averaging of the 3D site TCFs $h_{\alpha}^{ss}(\mathbf{r})$ to obtain the radial site–site TCFs $h_{\alpha\gamma}^{ss}(r)$, which is a numerically stable procedure. In contrast, the latter need first to orientationally average the 3D site DCFs $c_{\alpha}^{ss}(\mathbf{r})$, and then to decompose the averaged radial $\bar{c}_{\alpha\gamma}^{ss}(r)$ into the *partial* site–site DCFs $c_{\alpha\gamma}^{ss}(r)$ according to the additive approximation (19). As has been said, this is exact only in the asymptotic limit, and on the other hand, can cause numerical instability which has been observed by Cortis, Rossky, and Friesner³⁴ in the case of a liquid of highly charged polar molecules.

Numerical solution of a 3D integral equation constitutes a significant challenge. We converged the solvent–ion as well as solvent–solvent SC-3D-RISM/HNC integral equations by means of the modified direct inversion in the iterative subspace (MDIIS) method elaborated by Kovalenko, Ten-no, and Hirata.³⁷ It has been presented in detail in Refs.

37, 38, and 40, and so we only briefly sketch the basic iterative step used in computing the correlation functions. We solve the pure solvent set, Eqs. (9)–(11), for the 3D site indirect correlation function $t_\gamma^{ss}(\mathbf{r}) = h_\gamma^{ss}(\mathbf{r}) - c_\gamma^{ss}(\mathbf{r})$. Inserted into the HNC closure (10), it yields $g_\gamma^{ss}(\mathbf{r})$ and then $c_\gamma^{ss}(\mathbf{r})$. Thereafter we orientationally average $g_\gamma^{ss}(\mathbf{r})$ by using the resummation in reciprocal space (11) to obtain the radial site–site TCFs $h_{\alpha\gamma}^{ss}(r)$, and finally calculate $h_\gamma^{ss}(\mathbf{r})$ from the 3D-RISM equation (9). The vector residual of the SC-3D-RISM/HNC equations which is a functional to be zeroed in the process of solution, $R_\gamma^{ss}(\mathbf{r}) = R_\gamma^{ss}[\{t_\gamma^{ss}(\mathbf{r})\}]$, is defined as the difference of the 3D site TCFs following from the 3D-RISM equation and the 3D-HNC closure:³⁷

$$\begin{aligned} g_\gamma^{ss}(\mathbf{r}) &= \exp(-\beta u_\gamma^{ss}(\mathbf{r}) + t_\gamma^{ss}(\mathbf{r})), \\ h_{\alpha\gamma}^{ss}(r) &= \langle g_\gamma^{ss}(\mathbf{r}_{s\alpha} + \mathbf{r}) \rangle_{\Omega_r} - 1, \\ h_\gamma^{ss}(\mathbf{r}) &= \sum_\alpha (g_\alpha^{ss}(\mathbf{r}) - 1 - t_\alpha^{ss}(\mathbf{r})) * (\omega_{\alpha\gamma}^{ss}(r) + \rho h_{\alpha\gamma}^{ss}(r)), \\ R_\gamma^{ss}(\mathbf{r}) &= g_\gamma^{ss}(\mathbf{r}) - 1 - h_\gamma^{ss}(\mathbf{r}). \end{aligned} \quad (20)$$

Given the solvent–solvent correlations, the solvent–ion set, Eqs. (5)–(7), are solved similarly for the 3D solvent–ion indirect correlation function $t^{si}(\mathbf{r}) = h^{si}(\mathbf{r}) - c^{si}(\mathbf{r})$. The residual $R^{si}(\mathbf{r}) = R^{si}[\{t^{si}(\mathbf{r})\}]$ is setup by

$$\begin{aligned} g^{si}(\mathbf{r}) &= \exp(-\beta u^{si}(\mathbf{r}) + t^{si}(\mathbf{r})), \\ h_\alpha^{si}(\mathbf{r}) &= \langle g^{si}(\mathbf{r}_{s\alpha} + \mathbf{r}) \rangle_{\Omega_r} - 1, \\ h^{si}(\mathbf{r}) &= g^{si}(\mathbf{r}) - 1 - t^{si}(\mathbf{r}) + \rho \sum_\alpha c_\alpha^{ss}(\mathbf{r}) * h_\alpha^{si}(\mathbf{r}), \\ R^{si}(\mathbf{r}) &= g^{si}(\mathbf{r}) - 1 - h^{si}(\mathbf{r}). \end{aligned} \quad (21)$$

We start the MDIIS iterative procedure from the initial vector, on the one hand, possessing the long-range asymptotics of $t_\gamma^{ss}(\mathbf{r})$ which is essentially the electrostatic asymptotics of the DCF $c_\gamma^{ss}(\mathbf{r})$ but of opposite sign, and on the other hand, fitting its behavior inside the repulsive cores where it goes to a constant. It was first noticed by Ng⁴² that this delivers a very good estimate of the DCF for a one-component plasma. Such a guess represents a major part of the solution for charged molecular systems in both 1D and 3D cases, which allows us to begin convergence at once at given temperature and full molecular charge.^{36–40} We thus avoid the procedures of gradually decreasing temperature (the so-called “cooling”) and increasing site charges (“charging”) usually employed to facilitate convergence.^{9,10,34,43} This greatly reduces computational expenses. It should be noted that the sum of the bare Coulomb potentials of the point charges at the interaction sites is poor as the initial guess for the DCF. The latter follows the run of the interaction potential (with opposite sign) practically down to the bottom of the attractive well, after which it turns to the short-range behavior. The potential minimum usually results from the competition of the Coulomb attraction and the short-range repulsive core. Although it provides the correct asymptotics of the DCFs at long-range to cancel out with the interaction potential in the exponent of the HNC

closure, in the first peak region the Coulomb attraction substantially exceeds the well depth of the total interaction potential. This overflows the HNC exponent at the iteration start. Therefore, the initial guess of the DCF should include the Coulomb potential properly reduced in the region of the repulsive core. There are several functional forms of such “damping.”^{42,36–40} In the 3D case, it is conveniently related to the Ewald summation employed within the supercell technique to synthesize the electrostatic potential of a solute on the supercell grid. Namely, we specify the starting vector as the electrostatic potential of site charge q_γ in the field of the site charges of the labeled solvent molecule q_α but smeared by the Gaussian distribution to half-width σ

$$t_\gamma^{ss(0)}(\mathbf{r}) = \frac{\beta q_\gamma}{V_{\text{cell}}} \sum_{\mathbf{k} \neq 0} \sum_\alpha q_\alpha \frac{4\pi}{k^2} \exp\left(i\mathbf{k}(\mathbf{r} - \mathbf{r}_\alpha) - \frac{k^2 \sigma^2}{4}\right), \quad (22)$$

where V_{cell} is the supercell volume, and the summation over wave vector \mathbf{k} is carried out over its 3D grid values by means of the 3D-FFT. The initial guess for the solvent–ion correlation, $t^{si(0)}(\mathbf{r})$, is specified by the same expression (22) but for the ion charge q_i in the field of the smeared molecular charges q_α . The smearing parameter σ is to be roughly adjusted so as to provide a moderate value of the root mean square residual at start. Notice also that the MDIIS procedure can accidentally send the iterated vector far from the solution, and then it should be restarted from the iterated vector with the minimal residual.^{37,38,40} In order to avoid overflow of the HNC exponent is such a case, we put an upper limit of 10 on the exponent argument. This prevents overflow interruptions in the computational procedure while not influencing the converged distributions, for which it is well below this level.

III. THERMODYNAMICS OF SOLVATION

A close analytical expression for the solvation free energy has been derived within the OZ/HNC theory by Morita and Hiroike⁴⁴ and generalized to the RISM/HNC method by Singer and Chandler.⁴⁵ It can be trivially extended to the 3D-RISM/HNC approach.³⁸

Since we consider solvation of a single ion, below all excess thermodynamic quantities are implied in the limit of infinite dilution. The excess chemical potential of solvation of an ion in a molecular solvent is obtained by the common procedure of “switching on” the solute–solvent interaction, that can be written as

$$\Delta\mu = \rho \int d\mathbf{r} \int_0^{u^{si}(\mathbf{r})} \delta u^{si}(\mathbf{r}) g^{si}(\mathbf{r}). \quad (23)$$

If the 3D solvent–ion correlations are obtained from the MOZ/HNC equations (1) and (7), the integration over the interaction in (23) can be performed analytically. Substitution of the 3D solvent–ion indirect correlation function $t^{si}(\mathbf{r})$ from the MOZ equation (1) into the 3D-HNC closure (7)

$$h^{si}(r, \Omega) + 1 = \exp\left(-\beta u^{si}(r, \Omega) + \frac{\rho}{\Omega} \int d\mathbf{r}' d\Omega' c^{ss} \times (|\mathbf{r} - \mathbf{r}'|, \Omega, \Omega') h^{si}(r', \Omega')\right), \quad (24)$$

and functional variation of expression (24) gives after simple rearrangement

$$\begin{aligned} \beta g^{si}(r, \Omega) \delta u^{si}(r, \Omega) &= -\delta h^{si}(r, \Omega) + \frac{\rho}{\Omega} \int d\mathbf{r}' d\Omega' c^{ss} (|\mathbf{r} - \mathbf{r}'|, \Omega, \Omega') \\ &\times \delta h^{si}(r', \Omega') + h^{si}(r, \Omega) \frac{\rho}{\Omega} \int d\mathbf{r}' d\Omega' c^{ss} \\ &\times (|\mathbf{r} - \mathbf{r}'|, \Omega, \Omega') \delta h^{si}(r', \Omega'). \end{aligned} \quad (25)$$

On insertion into (23), the first and second terms of expression (25) can be immediately integrated over the interaction. Taking into account the MOZ equation (1), and adding integration over orientation Ω to symmetrize the third term, we have

$$\begin{aligned} \beta \Delta \mu^{\text{HNC}} &= -\rho \int d\mathbf{r} c^{si}(\mathbf{r}) \\ &+ \frac{\rho^2}{\Omega^2} \int d\mathbf{r} d\mathbf{r}' d\Omega d\Omega' \int_0^{u^{si}(\mathbf{r})} h^{si}(r, \Omega) c^{ss} \\ &\times (|\mathbf{r} - \mathbf{r}'|, \Omega, \Omega') \delta h^{si}(r', \Omega'). \end{aligned} \quad (26)$$

The last integral over the interaction in (26) is taken by using the symmetry of the variation

$$\begin{aligned} \delta(h^{si}(r, \Omega) c^{ss}(|\mathbf{r} - \mathbf{r}'|, \Omega, \Omega') h^{si}(r', \Omega')) &= \delta h^{si}(r, \Omega) c^{ss}(|\mathbf{r} - \mathbf{r}'|, \Omega, \Omega') h^{si}(r', \Omega') \\ &+ h^{si}(r, \Omega) c^{ss}(|\mathbf{r} - \mathbf{r}'|, \Omega, \Omega') \delta h^{si}(r', \Omega'). \end{aligned} \quad (27)$$

Using Eq. (1), this results in the expression for the chemical potential of solvation of the ion in the familiar closed analytical form

$$\Delta \mu^{\text{HNC}} = \rho kT \int d\mathbf{r} \left\{ \frac{1}{2} (h^{si}(\mathbf{r}))^2 - \frac{1}{2} h^{si}(\mathbf{r}) c^{si}(\mathbf{r}) - c^{si}(\mathbf{r}) \right\}. \quad (28)$$

In the present approach, we determine the 3D solvent-ion TCF from the 3D-RISM equation (5). Making functional variation of the 3D-RISM/HNC equation (8), and inserting the result into (23) with allowance for (5) gives

$$\begin{aligned} \beta \Delta \mu^{\text{HNC}} &= -\rho \int d\mathbf{r} c^{si}(\mathbf{r}) + \rho^2 \int d\mathbf{r} d\mathbf{r}' \int_0^{u^{si}(\mathbf{r})} h^{si}(\mathbf{r}) \\ &\times \sum_{\alpha} c_{\alpha}^{ss}(\mathbf{r} - \mathbf{r}') \delta h_{\alpha}^{si}(\mathbf{r}'). \end{aligned} \quad (29)$$

The latter term in this expression cannot be integrated analytically over the interaction since the variation

$$\begin{aligned} \delta(h^{si}(\mathbf{r}) c_{\alpha}^{ss}(\mathbf{r} - \mathbf{r}') h_{\alpha}^{si}(\mathbf{r}')) &= \delta h^{si}(\mathbf{r}) \sum_{\alpha} c_{\alpha}^{ss}(\mathbf{r} - \mathbf{r}') h_{\alpha}^{si}(\mathbf{r}') + h^{si}(\mathbf{r}) \\ &\times \sum_{\alpha} c_{\alpha}^{ss}(\mathbf{r} - \mathbf{r}') \delta h_{\alpha}^{si}(\mathbf{r}'), \end{aligned} \quad (30)$$

does not possess the symmetry as in Eq. (27). Nevertheless, taking into account the decomposition (2) employed in the derivation of the 3D-RISM integral equation (5), the second term of expression (29) is equivalent to that in (26), and the variation (30) is same as (27). Therefore, within the additive approximation (2), the solvation chemical potential obtained from the 3D-RISM/HNC equations (5) and (7) does take the form as in Eq. (28).

The excess energy of solvation can be obtained by taking the isochoric temperature derivative⁴⁶⁻⁴⁸

$$\Delta \varepsilon = \left(\frac{\partial(\beta \Delta \mu)}{\partial \beta} \right)_V = \Delta \mu + T \Delta s_V, \quad (31)$$

where Δs_V is the excess entropy at constant volume. An alternative decomposition of the excess chemical potential of solvation into the excess enthalpy Δh and the excess entropy Δs_P at constant pressure can be achieved by the use of the isobaric temperature derivative⁴⁹

$$\Delta h = \left(\frac{\partial(\beta \Delta \mu)}{\partial \beta} \right)_P = \Delta \mu + T \Delta s_P. \quad (32)$$

The difference between the two entropic terms is given by⁴⁸

$$T(\Delta s_P - \Delta s_V) = \Delta h - \Delta \varepsilon = T \alpha_P \rho \left(\frac{\partial \Delta \mu}{\partial \rho} \right)_T, \quad (33)$$

where $\alpha_P = (\partial(\log V)/\partial P)_P$ is the isobaric thermal expansion coefficient of solvent.

Applying Eq. (31) to the solvation chemical potential (28) yields the solvation energy in the form

$$\begin{aligned} \Delta \varepsilon &= \rho kT \int d\mathbf{r} \beta u^{si}(\mathbf{r}) g^{si}(\mathbf{r}) \\ &+ \frac{1}{2} \rho kT \int d\mathbf{r} \{ c^{si}(\mathbf{r}) \delta_T h^{si}(\mathbf{r}) - h^{si}(\mathbf{r}) \delta_T c^{si}(\mathbf{r}) \}, \end{aligned} \quad (34)$$

where $\delta_T f^{si}(\mathbf{r}) = T(\partial f^{si}(\mathbf{r})/\partial T)_P$ (f^{si} stands for c^{si} and h^{si}) are the temperature derivatives of the 3D correlation functions. Although they can be obtained by solving integral equations derived by differentiation of the RISM/HNC ones,^{25,47,48} we found it is much simpler to calculate them directly by using the central finite differencing approximation

$$\delta_T f^{si}(\mathbf{r}) \approx T \frac{f^{si}(\mathbf{r}; T + \Delta T) - f^{si}(\mathbf{r}; T - \Delta T)}{2\Delta T}. \quad (35)$$

In expression (34), the former term is the average solute-ion interaction energy, and the latter is the solvent reorganization energy.

The solvation enthalpy obtained from Eqs. (33) and (34) is written as

$$\Delta h = \Delta \varepsilon + T \alpha_p \left[\Delta \mu^{\text{HNC}} + \frac{1}{2} \rho k T \int d\mathbf{r} \{ h^{si}(\mathbf{r}) \delta_\rho c^{si}(\mathbf{r}) - c^{si}(\mathbf{r}) \delta_\rho h^{si}(\mathbf{r}) \} \right], \quad (36)$$

where $\delta_\rho f^{si}(\mathbf{r}) = \rho (\partial f^{si}(\mathbf{r}) / \partial \rho)_\rho$ are the temperature derivatives of the 3D correlation functions, and are calculated by the central finite differencing as in Eq. (35).

IV. ELECTROSTATIC CORRECTIONS FOR FINITE SIZE OF THE SUPERCELL

The SC-3D-RISM approach requires special treatment for the electrostatic asymptotics of the correlation functions, representing ordering of polar molecular solvent in the presence of an ion. However, they are somewhat different from the case of the 3D-RISM/HNC equations for the correlations of polar molecular solvent sites around an ionic solute,⁴⁰ because we instead consider those of an ion around one polar solvent molecule regarded as a solute. The 3D solvent–ion DCF now has the asymptotics of an ion–dipole rather than Coulomb potential,

$$c^{si(lr)}(\mathbf{r}) = -\beta \Phi^{si}(\mathbf{r}) = -\beta q_i \sum_\alpha \frac{q_\alpha}{|\mathbf{r} - \mathbf{r}_\alpha|} \sim -\beta q_i \frac{\mathbf{d}_s \cdot \mathbf{r}}{r^2}, \quad (37)$$

where q_i is the ion charge, and $\mathbf{d}_s = \sum_\alpha q_\alpha \mathbf{r}_\alpha$ is the dipole moment of a solvent molecule comprising site charges q_α . Moreover, it is obvious from the definition of the potential of mean force, $w^{si}(\mathbf{r}) \equiv -kT \log(g^{si}(\mathbf{r})) \sim -kTh^{si}(\mathbf{r})$, that the 3D solvent–ion TCF has a similar ion–dipole asymptotics but scaled by the dielectric screening. It is the long-range asymptotics of the potential of mean force between the molecular dipole and the ion in a dielectric continuum

$$h^{si(lr)}(\mathbf{r}) = -\beta \Phi^{si}(\mathbf{r}) / \epsilon_{\text{RISM}}, \quad (38)$$

where ϵ_{RISM} is the dielectric constant of solvent in the RISM description.

The solvent–ion SC-3D-RISM/HNC equations (5)–(7) together with the solvent–solvent ones (9)–(10) yield the same trivial dielectric constant as that following from the conventional 1D-RISM/HNC theory^{6,13,50}

$$\epsilon_{\text{RISM}} = 1 + \frac{4}{3} \pi \beta \rho d_s^2. \quad (39)$$

This is essentially a result of the fact that the 3D-HNC approximation (10) is applied to 3D *site* correlations that involve orientational averaging. The latter enforces an ion–dipole asymptotics of the solvent 3D site DCFs $c_\alpha^{ss}(\mathbf{r})$. It leads to the above trivial dielectric constant ϵ_{RISM} by the solvent route when inserted into the solvent–solvent 3D-RISM integral equation (9), and further by the solute route from the solute–solvent 3D-RISM equation (5). Perkyns and Pettitt¹⁵ showed that the 1D-RISM theory prediction for the dielectric constant can be essentially improved by introduction of bridge corrections to the solvent–solvent correlations, ensuring the dielectric consistency of the RISM approach. As a straightforward extension, Kovalenko and Hirata⁴⁰ have

adapted this correction to the 3D-RISM/HNC theory for an ionic molecular solute in a polar molecular solvent. The SC-3D-RISM approach at hand can be improved in a similar manner. We postpone a detailed consideration of its dielectric properties and elaboration of such a dielectric correction to future works.

The SC-3D-RISM/HNC integral equations are solved by means of the supercell technique, and the electrostatic part of the 3D periodic potential $u^{si(p)}(\mathbf{r})$ between the ion and the periodic supercell images of the labeled solvent molecule is calculated by means of the Ewald summation method⁵¹

$$\Phi^{si(p)}(\mathbf{r}) = \frac{q_i}{V_{\text{cell}}} \sum_{\mathbf{k} \neq 0} \sum_\alpha q_\alpha \frac{4\pi}{k^2} \exp\left(i\mathbf{k} \cdot (\mathbf{r} - \mathbf{r}_\alpha) - \frac{k^2 \delta^2}{4}\right) + q_i \sum_\alpha q_\alpha \frac{1 - \text{erf}(\Delta r_\alpha / \delta)}{\Delta r_\alpha}, \quad (40)$$

where V_{cell} is the supercell volume, the summation over wave vector \mathbf{k} is carried out over its 3D grid values by means of the 3D-FFT, and δ is the half-width of Gaussian smearing of site charges q_α of the solvent molecule. Because the compensating charge potential decays on length δ which is typically much smaller than the supercell size, its direct-space summation over the periodic images of the solute is replaced in (40) with tabulation on the supercell grid, with separation Δr_2 from molecular site α determined subject to the minimum image convention,⁵¹ $\Delta r_{j,\alpha} = \min(\mathbf{r}_j - \mathbf{r}_{j,\alpha} + n_j L_j)$, $j = x, y, z$. Within this supercell treatment, the 3D solvent–ion DCF and TCF acquire the *periodic* long-range asymptotics

$$c^{si(plr)}(\mathbf{r}) = -\beta \Phi^{si(p)}(\mathbf{r}), \quad (41)$$

$$h^{si(plr)}(\mathbf{r}) = -\beta \Phi^{si(p)}(\mathbf{r}) / \epsilon_{\text{RISM}}. \quad (42)$$

Hünenberger and McCammon⁵² found for computer simulations that an artificial periodicity imposed by the use of the Ewald or related methods produces significant errors in the solvation free energy of an ion in a dielectric continuum. Kovalenko and Hirata⁴⁰ showed that for an ionic solute in polar molecular solvent, the distortion of the 3D solute–solvent correlation functions brought about by the 3D-RISM supercell treatment results in essential mistreatment of the solvation thermodynamics. For instance, the error in the solvation chemical potential of a univalent simple ion in ambient water amounts to 35 kcal/mol,⁴⁰ which is close to the effect of the periodicity artifact in molecular-dynamics simulations for a similar system.⁵³ It can be canceled out with an accuracy of better than 0.05 kcal/mol by introducing corrections to the 3D-RISM/HNC equations, restoring the asymptotics of the 3D solute–solvent site TCFs as well as DCFs.⁴⁰ The former is corrected for the a constant shift brought about by the supercell background charge density neutralizing the solute charge, and the latter for periodicity distorting the Coulomb asymptotics of the 3D solute–solvent site potential.

After solving the SC-3D-RISM/HNC equations (5), (6), (7) for $c^{si(p)}(\mathbf{r})$ and $h^{si(p)}(\mathbf{r})$ on the periodic supercell, the *nonperiodic* asymptotics of the 3D solvent–ion DCF is re-

stored merely by subtracting the electrostatic periodic potential (40) and adding back the theoretical expression (37)

$$c^{si}(\mathbf{r}) = c^{si(p)}(\mathbf{r}) + \beta(\Phi^{si(p)}(\mathbf{r}) - \Phi^{si}(\mathbf{r})). \quad (43)$$

The asymptotics (37) of the 3D solvent–ion TCF is restored in a somewhat different way so as to keep proper decay of the 3D solvent–ion distribution function at the repulsive core edge

$$g^{si}(\mathbf{r}) = g^{si(p)}(\mathbf{r}) \exp(\beta(\Phi^{si(p)}(\mathbf{r}) - \Phi^{si}(\mathbf{r}))/\epsilon_{\text{RISM}}). \quad (44)$$

The asymptotic correction $\Phi^{si(p)}(\mathbf{r}) - \Phi^{si}(\mathbf{r})$ is essential at a large separation between the solvent molecule and ion, and rapidly falls off inside the solvent–ion repulsive core. However, when introduced as an additive term rather than a factor in the distribution function, it results in a big error in the internal energy obtained by the integration of the solvent–ion distribution function with the interaction potential (34). Notice also that unlike polar molecular solvent around an ionic solute,⁴⁰ in the present case there is no need to correct the 3D solvent–ion TCF for the constant shift because the net charge of the labeled solvent molecule being the solute is zero and so the supercell neutralizing background is absent.

With the ion–dipole asymptotics (37) and (38), calculation of the solvation chemical potential from expression (28) requires analytical treatment of the long-range contributions. They appear in the both terms $h^{si}(\mathbf{r})c^{si}(\mathbf{r})$ and $(h^{si}(\mathbf{r}))^2$ but cancel out in $c^{si}(\mathbf{r})$ due to the solvent molecule electroneutrality. On separating out the electrostatic contribution, the rest of the integral is taken just over the supercell space on which the 3D correlation functions are defined

$$\begin{aligned} \Delta\mu^{\text{HNC}} = \Delta\mu^{(es)} + \rho kT \int_{V_{\text{cell}}} d\mathbf{r} & \left\{ \frac{1}{2} (h^{si}(\mathbf{r}))^2 \right. \\ & - \frac{1}{2} h^{si}(\mathbf{r})c^{si}(\mathbf{r}) - c^{si}(\mathbf{r}) \\ & \left. + \frac{\epsilon_{\text{RISM}} - 1}{2\epsilon_{\text{RISM}}^2} (\beta\Phi^{si(b)}(\mathbf{r}))^2 \right\}. \quad (45) \end{aligned}$$

To provide convergence of the electrostatic term $\Delta\mu^{(es)}$, we define the long-range asymptotic term as the electrostatic potential of broadened site charges rather than (37)

$$\Phi^{si(b)}(\mathbf{r}) = q_i \sum_{\alpha} \frac{q_{\alpha} \text{erf}(|\mathbf{r} - \mathbf{r}_{\alpha}|/\delta)}{|\mathbf{r} - \mathbf{r}_{\alpha}|}. \quad (46)$$

The long-range component

$$\begin{aligned} \Delta\mu^{(es)} &= -\frac{\epsilon_{\text{RISM}} - 1}{2\epsilon_{\text{RISM}}^2} \rho kT \int d\mathbf{r} (\beta\Phi^{si(b)}(\mathbf{r}))^2 \\ &= -\frac{\epsilon_{\text{RISM}} - 1}{2\epsilon_{\text{RISM}}^2} I^{(es)}, \quad (47) \end{aligned}$$

is then reduced, with allowance for the electroneutrality of the solvent molecule, to the one-dimensional integral

$$\begin{aligned} I^{(es)} &= 8\rho\beta q_i^2 \sum_{\alpha\gamma} q_{\alpha} q_{\gamma} \int_0^{\infty} dk \frac{\exp(-k^2\delta^2/2)}{k^2} \\ &\quad \times \left(\frac{\sin(kl_{\alpha\gamma})}{kl_{\alpha\gamma}} - 1 \right), \quad (48) \end{aligned}$$

which is easily evaluated by numerical integration.⁴¹

In a similar way, the ion solvation energy (34) with the correction for the finite size of the supercell is written as

$$\begin{aligned} \Delta\epsilon &= \Delta\epsilon^{(es)} + \rho kT \int_{V_{\text{cell}}} d\mathbf{r} \left\{ \beta u^{si}(\mathbf{r}) g^{si}(\mathbf{r}) \right. \\ &\quad + \frac{1}{2} (c^{si}(\mathbf{r}) \delta_T h^{si}(\mathbf{r}) - h^{si}(\mathbf{r}) \delta_T c^{si}(\mathbf{r})) \\ &\quad \left. + \frac{\epsilon_{\text{RISM}} + 1}{2\epsilon_{\text{RISM}}^2} (\beta\Phi^{si(b)}(\mathbf{r}))^2 \right\}, \quad (49) \end{aligned}$$

where $\delta_T c^{si}(\mathbf{r})$ and $\delta_T h^{si}(\mathbf{r})$ are the temperature derivatives of the corrected 3D correlation functions (43) and (44), calculated by using the finite differences (35). The electrostatic term in the solvation energy obtained on separating out the ion–dipole asymptotics (46) in the 3D correlation functions and their derivatives entering (49) has the form

$$\Delta\epsilon^{(es)} = -\frac{\epsilon_{\text{RISM}} + 1}{2\epsilon_{\text{RISM}}^2} I^{(es)}, \quad (50)$$

where the temperature derivative of the dielectric constant (39) is taken into account.

Finally, the ion solvation enthalpy (36) is corrected as

$$\begin{aligned} \Delta h &= \Delta\epsilon + \rho kT^2 \alpha_P \int_{V_{\text{cell}}} d\mathbf{r} \left[\frac{1}{2} (h^{si}(\mathbf{r}))^2 - \frac{1}{2} h^{si}(\mathbf{r})c^{si}(\mathbf{r}) \right. \\ &\quad \left. - c^{si}(\mathbf{r}) + \frac{1}{2} \{ h^{si}(\mathbf{r}) \delta_{\rho} c^{si}(\mathbf{r}) - c^{si}(\mathbf{r}) \delta_{\rho} h^{si}(\mathbf{r}) \} \right], \quad (51) \end{aligned}$$

where $\Delta\epsilon$ is the corrected solvation energy (49), whereas no electrostatic correction is necessary to the latter integral since its electrostatic components canceled out.

V. NUMERICAL RESULTS AND DISCUSSION

In order to test the SC-3D-RISM/HNC integral equation theory, we calculated the solvation structure and thermodynamics of the sodium and chlorine ions at infinite dilution in ambient water at temperature $T = 298$ K and density $\rho_{\text{water}} = 0.03334 \text{ \AA}^{-3}$. We employed the Extended Simple Point Charge (SPC/E) water model of Berendsen and co-workers.⁵⁴ The ion–water site as well as water site–site interactions are modeled by the sum of the Coulomb and 12-6 Lennard-Jones (LJ) potentials, with the LJ diameter and energy parameters determined by the standard Lorentz–Berthelot mixing rules. Following Pettitt and Rossky,¹² a LJ size of 0.4 \AA is introduced for the water hydrogen sites. This does not affect the entire potential a water molecule since the hydrogens are situated well inside the oxygen core, however allows one to adjust the RISM description for hydrogen bonds. For the ions, we adopted the LJ parameters elaborated

by Dang and co-workers.⁵⁵ The latter have been used by Rasaiah and co-workers in molecular simulations.^{53,56}

The 3D treatment was done on a grid of 64^3 points in a cubic supercell of sufficiently large size of 25.6 \AA to include three hydration shells around the ion. The increase of the grid resolution to 128^3 points results in a negligible refinement of the hydration chemical potential. The smearing parameter δ in Eqs. (40), (46), and (48) was chosen to be 2.5 \AA . For the solvent-solvent and solvent-ion initial vectors, the smearing parameter in Eq. (22) was taken as $\sigma=1$ and 1.8 \AA , respectively. This provides at start the root-mean-square residual of magnitude less than one, which ensures fast and stable convergence. In calculation of the temperature derivatives of the 3D correlation functions in (49) by the finite differences (35), the temperature step-size ΔT is 2 K, and the density derivatives in (51) were obtained in the same way with the density step-size $\Delta\rho$ to be 0.0002 \AA^{-3} .

With the use of the MDIIS method,^{37,38,40} the solvent-solvent integral equations (20) at given temperature and density are converged to a root-mean-square accuracy of 10^{-5} in 80 iterations with the MDIIS subspace of 10 vectors, which for the 3D grid of 64^3 points takes about 12 min on a 600 MHz Pentium PC. Solution of the solvent-ion integral equations (21) requires 30 MDIIS iterations and takes about 1.5 min.

The ion-solvent site radial distributions are finally obtained from (4a) by explicit numerical orientational averaging of the 3D ones in direct space. We calculated the integral over sphere by employing the 700-point set of the Repulsion scheme within the Spherical Harmonic Reduction or Elimination by a Weighted Distribution (SHREWD) quadrature method.⁵⁷

Figure 1 exhibits the radial distribution functions between the water interaction sites and the Cl^- ion, obtained from the SC-3D-RISM/HNC procedure, and the 1D-RISM/HNC approach as well as the molecular simulations for the system with the same potential parameters.⁵³ It is evident that as compared to the conventional 1D-RISM theory, the 3D treatment at hand does essentially improve the prediction of the positions of the first and second solvation shell peaks and the minima. Notice that the unphysical penetration of water hydrogen sites towards the negatively charged Cl^- ion, typical for the former is completely eliminated in the latter. The extrema of the hydrogen-chlorine distribution now fit well the simulation results. The position of the first peak of the oxygen-chlorine distribution is significantly improved too, and the second peak is much better formed and situated closer to the simulation data. This demonstrates the improved description of the orientational ordering of water molecules in the ion solvation shell. As a shortcoming, the present 3D approach underestimates amplitude of the solvation shell oscillations. To treat this point requires to add bridge corrections to the molecular 3D-HNC closure (7). Lombardero and co-workers have shown for molecular liquids^{27,58} and molecular mixtures⁵⁹ that the predictions of the MOZ equation can be significantly improved by applying a generalization of the reference hypernetted chain (RHNC) closure⁶⁰ with Verlet's modified approximation.⁶¹ This would refine the description of the solvent-ion distributions

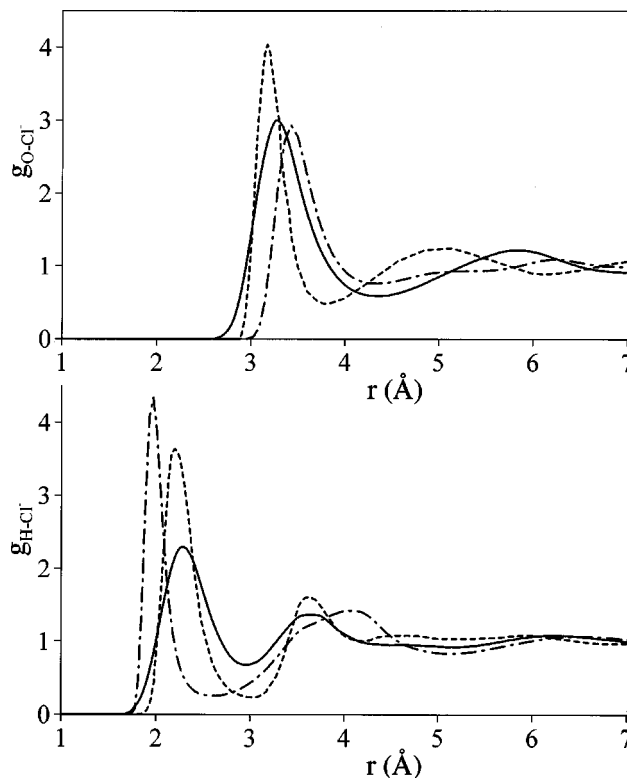


FIG. 1. Radial distribution functions between the Cl^- ion and the oxygen and hydrogen interaction sites of water solvent molecules, $g_{\text{O-Cl}}(r)$ and $g_{\text{H-Cl}}(r)$, at ambient conditions. Comparison of the orientational averages of the 3D water-ion distribution function $g_{\text{w-Cl}}(\mathbf{r})$ obtained from the SC-3D-RISM/HNC theory with those following from the conventional, 1D-RISM/HNC approach, and the molecular simulations (Ref. 53) (solid, dash-dotted, and short-dashed lines, respectively).

in the contact region which gives a significant contribution to the solvation free energy. It should be noted, however, that for liquids with strong hydrogen bonding like water and methanol, the effect of these bridge corrections on the ion solvation structure is questionable. Lombardero and co-workers,³⁰ and Richardi, Millot, and Fries²⁹ also found that the use of the hard-sphere bridge functions within the MOZ/RHNC approach scarcely affects both the structure and thermodynamic properties of these liquids at ambient conditions. They reasonably attributed this failure to the shape discrepancy between the spherically symmetric bridge functions of hard spheres which form closely packed structures, and the local geometry of loosely coordinated liquid like ambient water showing tetrahedral ordering. Nevertheless, this conclusion should be applied to an ion hydration shell with caution, and encourages further investigation and search for bridge functions incorporating those geometric features.

Figure 2 makes a comparison of the radial distribution functions for the water interaction sites and the Na^+ ion. There is some improvement for the first peak height of the hydrogen-sodium distribution in the 3D approach against the 1D-RISM treatment, whereas the predicted height of the oxygen-sodium peak is worsened. Notice, however, that the oxygen peak in the SC-3D-RISM approach is noticeably wider. This yields the oxygen running coordination number of the first solvation shell $N_{\text{O-Cl}}^{(3\text{D-RISM})} = 4.9$, which is higher

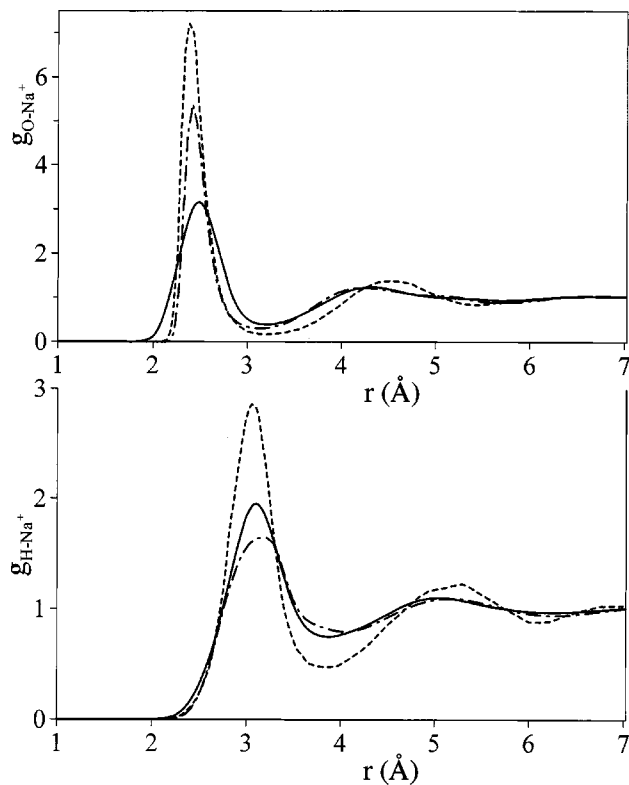


FIG. 2. Same as in Fig. 1, but for the Na^+ ion.

than the value $N_{\text{O-Cl}^-}^{(\text{RISM})} = 4.4$ following from the 1D-RISM method, and is closer to the simulation one $N_{\text{O-Cl}^-}^{(\text{MD})} = 5.8$. Again, the agreement with simulations could be improved by employing bridge corrections, as discussed above for the water–chlorine radial distributions.

Beside the radial distribution functions of solvent sites around the ion, the SC-3D-RISM approach provides the orientational dependence of solvent molecules. Equally, it can be seen as a 3D spatial distribution function of the ion around the labeled solvent molecule. Figure 3 shows sections of the 3D distribution of the Cl^- ion around a water molecule, passing through its oxygen. Water oxygens form the first and second solvation shells around the Cl^- ion that are of small height about 1.2–1.6 almost everywhere, except for the high narrow peaks at the arrangements with the ion located in front of one of the water hydrogens. The first and second peaks at these positions reach respectively $g_{\text{W-Cl}^-}^{(\text{max1})} = 73.7$ and $g_{\text{W-Cl}^-}^{(\text{max2})} = 3.0$, even the latter higher than the rest of the solvation shell. The two peaks are attributed to the formation of solvation structures of water molecules hydrogen-bonded to the Cl^- ion due to the asymmetry of the electrostatic field of a water molecule, well known from the 1D-RISM/HNC^{22,25} and 3D-RISM/HNC treatment⁴⁰ as well as simulations.^{53,65,66} The SC-3D-RISM/HNC theory substantially improves the predicted positions of the hydrogen bonding. On orientational averaging, these narrow peaks turn into the much lower first peaks of the chlorine–water oxygen and hydrogen radial distributions of height $g_{\text{O-Cl}^-}^{(\text{max1})} = 3.0$ and $g_{\text{W-Cl}^-}^{(\text{max2})} = 2.3$ (Fig. 1 and 2). The saddle point between the two maxima of the first solvation shell (upper plot in Fig. 3) still

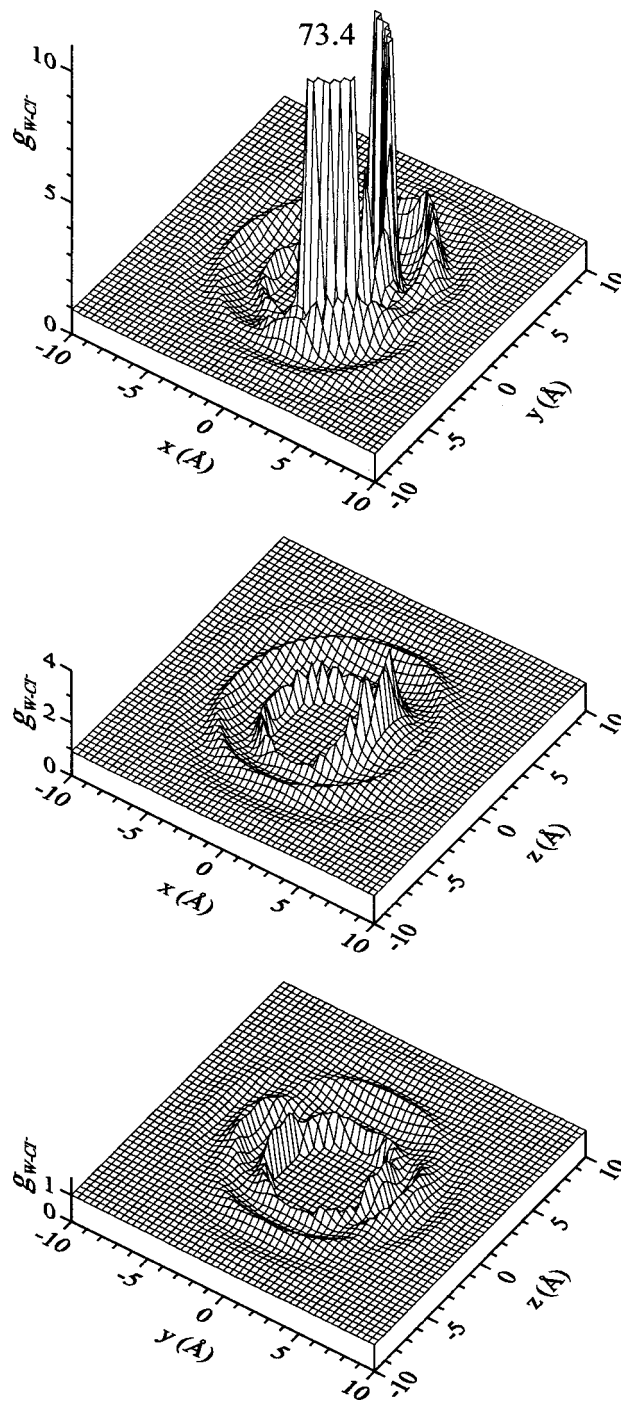


FIG. 3. Three-dimensional distribution function between the labeled water molecule and the Cl^- ion, $g_{\text{W-Cl}^-}(\mathbf{r})$, following from the SC-3D-RISM/HNC theory for the ion in ambient water. Sections of the 3D water–ion distribution in the orthogonal planes XOY , XOZ , and YOZ passing through the oxygen site (upper, middle, and lower plots, respectively). The number at the peaks shows their height. The water molecule is situated in plane XOY , and its dipole moment is directed along axis OX . The oxygen and hydrogen interaction sites have Cartesian coordinates $\mathbf{r}_\text{O} = (0,0,0)$ Å and $\mathbf{r}_\text{H} = (0.5774, \pm 0.8165, 0)$ Å.

has a relatively large value of about $g_{\text{W-Cl}^-} = 4$ (seen as a peak in the middle plot).

The 3D distribution of the Na^+ ion around a water molecule is depicted in Fig. 4. It has a single large maximum $g_{\text{W-Na}^+}^{(\text{max1})} = 50.3$ corresponding to the arrangement with the

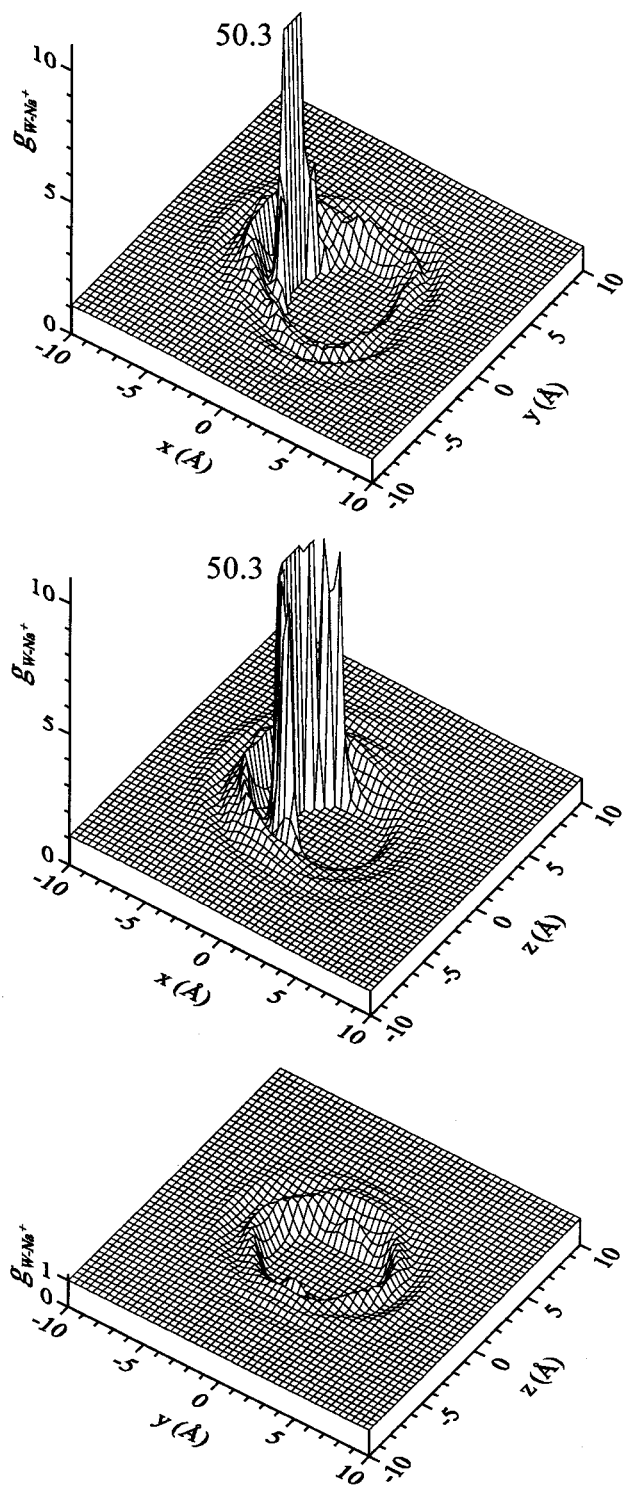


FIG. 4. Same as in Fig. 3, but for the Na^+ ion.

Na^+ ion facing the water oxygen. The second shell peak reaches height $g_{\text{W-Na}^+}^{(\text{max}2)} = 2.8$. Notice that the first peak is narrow in the molecular plane where it is concentrated mainly at the Ox axis (upper plot), whereas it becomes a wide “arc” stretched over the oxygen in perpendicular to the molecule plane (middle plot). Again, such arrangements of the Na^+ ion on the arc around the oxygen correspond to the directions usually occupied by hydrogen bonds around a water molecule in uniform ambient water. Unlike the hydrogen bond-

ing to Cl^- , water molecules show a simple dipole-like orientation around the Na^+ ion. The two small subpeaks in the lower plot section of the first hydration shell are just the YOZ -sections of the arc ends.

The hydration thermodynamics of the Cl^- and Na^+ ions in ambient water is shown in Table I. The comparison reveals a qualitative agreement of both the 1D-RISM/HNC and the SC-3D-RISM/HNC approaches with the simulations and experiment. It follows from both integral equation theory^{22,25,47,48} and simulations^{53,55,56,65–69} of hydration of simple ions that its thermodynamics as well as structure are very sensitive to the details of the ion potentials, such as softness of the ion repulsive core. With the appropriate choice of the parameters for the site–site interactions, Yu, Roux, and Karplus⁴⁸ achieved a good agreement between the 1D-RISM/HNC theory and experiment. Our goal, however, is to show the superiority of the SC-3D-RISM theory over the site–site one rather than to fit to experimental data by adjusting the parameters. It is evident that the 3D treatment noticeably improves the prediction of the solvation energy and chemical potential as compared to the conventional site–site approach, which is very sensitive to the behavior of the solute–solvent distributions in the repulsive core region. This also results in a noticeable improvement for the both hydration entropies, Δs_V and Δs_P , prone to errors as a difference between close values calculated. Further improvement can be obtained by refining the parameters of the ion–water potentials as well as by employing dielectric corrections. Yu, Roux, and Karplus⁴⁸ showed that the simple dielectric correction in the form of scaling the site–site Coulomb potential by a constant^{10,70,71} brings the thermodynamics of ionic hydration closer to the experimental values. As has been discussed above, a proper way within a 3D-RISM theory for an ion–molecular liquid⁴⁰ is to employ the consistent dielectric corrections of Perkyns and Pettitt.¹⁵ For the SC-3D-RISM/HNC approach, this will be done in future work.

VI. CONCLUSION

We have elaborated a self-consistent 3D-RISM/HNC integral equation theory for simple ions at infinite dilution in a polar molecular solvent. The main advantage of the SC-3D-RISM approach is that it eliminates the inconsistency in the positions of the ion–solvent site distribution peaks. The latter is related to the problem of “auxiliary sites” in the conventional, 1D-RISM/HNC theory, and arises due to a strong alignment of solvent molecules in the solvation shell around the ion attracting the solvent molecule sites of opposite charge. The better description of the ion–solvent distribution functions improves the predictions for the solvation thermodynamics as well. We tested the proposed theory by the example of hydration of the Na^+ and Cl^- ions in ambient water at infinite dilution. The hydration structure obtained from the SC-3D-RISM/HNC theory shows a substantially better agreement with simulations than that following from the 1D-RISM/HNC approach. A noticeable improvement of the predictions for the hydration thermodynamics is also observed.

The SC-3D-RISM/HNC theory can be further advanced

TABLE I. Thermodynamics of solvation of the Cl^- and Na^+ ions in ambient water.

Approach	$\Delta\mu$ ($\Delta\mu^{(es)}$) ^a (kcal/mol)	$\Delta\epsilon$ ($\Delta\epsilon^{(es)}$) ^a (kcal/mol)	Δh (kcal/mol)	Δs_V (cal/mol)	Δs_P (cal/mol)
Cl^-					
SC-3D-RISM/HNC	-79.5 (-48.5) ^a	-93.5 (-53.7) ^a	-98.9	-47.0	-64.8
1D-RISM/HNC	-83.9	-100.1	-105.7	-54.3	-73.0
MD ^b	-86.0			-16.	
experiment	-80.5 ^c		-88.2 ^c	-20.1 ^e	-25.8 ^c
	-73.9 ^d		-81.8 ^d		-26.5 ^d
Na^+					
SC-3D-RISM/HNC	-80.1 (-48.5) ^a	-90.2 (-53.7) ^a	-95.6	-34.0	-52.0
1D-RISM/HNC	-77.3	-88.8	-94.1	-38.6	-56.4
MD ^b	-82.9			-14.	
experiment	-89.6 ^c		-99.9 ^c	-23.8 ^e	-34.5 ^c
	-96.4 ^d		-106.6 ^d		-34.2 ^d

^aValues in parentheses are the electrostatic contributions in the excess chemical potential and energy of hydration, given by expressions (47) and (50), respectively.

^bFrom Reference 53.

^cFrom Reference 62.

^dFrom Reference 63.

^eFrom Reference 64.

in a number of points. It can be readily generalized to the case of finite ionic concentrations by including ions into the solvent surrounding the labeled solvent molecule and ion. This requires the consistent dielectric corrections of Perkyns and Pettitt¹⁵ to be employed to provide a consistent description of the dielectric properties of ion-molecular solution, similarly to their generalization to the 3D-RISM/HNC case.⁴⁰ Such a dielectric correction would improve the predicted solvation thermodynamics as well. Finally, it seems to be worthwhile to modify the molecular 3D-HNC closure for the 3D solvent-ion correlations by using the molecular generalization of Verlet's modified bridge corrections⁶¹ within the RHNC approach.⁶⁰ This would improve the description of the solvent-ion distributions in the contact region which gives a significant contribution to the solvation free energy. However, for solvents with strong hydrogen bonding ordering like ambient water and methanol, appropriate bridge functions are required which would allow for the local geometry of the ordering.

With a refinement of the potential parameters as well as these modifications, the SC-3D-RISM treatment could provide the description of the structure and thermodynamics of solvation of simple ions in a good agreement with experiment. On the other hand, it can be used to elaborate a functional form of bridge corrections necessary to improve the SC-3D-RISM treatment of a polar molecular liquid, and to extend it to the case of molecular ions. Such short-range bridge corrections would be advantageous for modification of the 1D-RISM/HNC theory as well. The latter is essentially simpler and faster than the 3D-RISM treatment, and thus is much easier to combine with MC simulated annealing⁷² or generalized-ensemble MC simulation methods.^{73,74} This can provide a powerful and efficient tool for reliable prediction of conformations of biomolecules with due account for the water solvent effect at the microscopic level.^{11,72} For hydration of hydrophobic molecular solutes, the predictive capabilities of the RISM/HNC theory can be significantly improved by adding the repulsive bridge correction (RBC).²⁴

The proposed SC-3D-RISM approach would allow one to elaborate short-range bridge corrections to the RISM theory for charged and polar molecular solutes.

ACKNOWLEDGMENTS

This research was supported by the National Science Foundation and a generous gift from Dow Chemical Company. A.K. is grateful to Professor Fumio Hirata for stimulating discussions.

- ¹*Mechanism of Protein Folding*, edited by R. H. Pain (Springer, New York, 1994).
- ²T. E. Creighton, *Proteins: Structure and Molecular Properties* (Freeman, New York, 1993).
- ³M. H. Werner, A. M. Gronenborn, and G. M. Clore, *Science* **271**, 778 (1996).
- ⁴M. T. Record, Jr., S. J. Mazur, P. Melancon, J. H. Roe, S. L. Shaner, and L. Unger, *Annu. Rev. Biochem.* **50**, 997 (1981).
- ⁵J. C. Gil Montoro and J. L. F. Abascal, *J. Chem. Phys.* **109**, 6200 (1998).
- ⁶J. P. Hansen and I. R. McDonald, *Theory of Simple Liquids* (Academic, London, 1976).
- ⁷D. Chandler and H. C. Andersen, *J. Chem. Phys.* **57**, 1930 (1972).
- ⁸F. Hirata and P. J. Rossky, *Chem. Phys. Lett.* **83**, 329 (1981).
- ⁹F. Hirata, B. M. Pettitt, and P. J. Rossky, *J. Chem. Phys.* **77**, 509 (1982).
- ¹⁰F. Hirata, P. J. Rossky, and B. M. Pettitt, *J. Chem. Phys.* **78**, 4133 (1983).
- ¹¹F. Hirata, *Bull. Chem. Soc. Jap.* **71**, 1483 (1998); and references therein.
- ¹²B. M. Pettitt and P. J. Rossky, *J. Chem. Phys.* **77**, 1451 (1982).
- ¹³J. S. Høye and G. Stell, *J. Chem. Phys.* **65**, 18 (1976).
- ¹⁴D. E. Sullivan and C. G. Gray, *Mol. Phys.* **42**, 443 (1981).
- ¹⁵J. S. Perkyns and B. M. Pettitt, *Chem. Phys. Lett.* **190**, 626 (1992); *J. Chem. Phys.* **97**, 7656 (1992).
- ¹⁶G. Hummer and D. M. Soumpasis, *Mol. Phys.* **75**, 633 (1992).
- ¹⁷C. S. Hsu, D. Chandler, and L. J. Lowden, *Chem. Phys.* **14**, 213 (1976).
- ¹⁸P. T. Cummings, C. G. Gray, and D. E. Sullivan, *J. Phys. A* **14**, 1483 (1981).
- ¹⁹J. S. Perkyns and B. M. Pettitt, *J. Phys. Chem.* **100**, 1323 (1996).
- ²⁰M. Kinoshita and F. Hirata, *J. Chem. Phys.* **106**, 5202 (1997).
- ²¹L. Lue and D. Blankschtein, *J. Phys. Chem.* **96**, 8582 (1992).
- ²²B. M. Pettitt, and P. J. Rossky, *J. Chem. Phys.* **84**, 5836 (1986).
- ²³Q. Du, D. Beglov, and B. Roux, *J. Phys. Chem. B* **104**, 796 (2000).
- ²⁴A. Kovalenko and F. Hirata, *J. Chem. Phys.* (to be published).
- ²⁵S.-H. Chong and F. Hirata, *J. Phys. Chem. B* **101**, 3209 (1997).
- ²⁶L. Blum and A. J. Torruella, *J. Chem. Phys.* **56**, 303 (1972).
- ²⁷C. Martín, E. Lomba, M. Lombardero, F. Lado, and J. S. Høye, *J. Chem.*

- Phys. **100**, 1599 (1994); C. Martín, M. Lombardero, M. Alvarez, and E. Lomba, *ibid.* **102**, 2092 (1995); F. Lado, E. Lomba, and M. Lombardero, *ibid.* **103**, 481 (1995); M. Alvarez, F. Lado, E. Lomba, M. Lombardero, and C. Martín, *ibid.* **107**, 4642 (1997).
- ²⁸ J. Richardi, P. H. Fries, and H. Krienke, Chem. Phys. Lett. **115**, 273 (1997); J. Richardi, P. H. Fries, R. Fischer, S. Rast, and H. Krienke, J. Mol. Liq. **73&74**, 465 (1997); Mol. Phys. **93**, 925 (1998).
- ²⁹ J. Richardi, C. Millot, and P. H. Fries, J. Chem. Phys. **110**, 1138 (1999).
- ³⁰ M. Lombardero, C. Martín, S. Jorge, F. Lado, and E. Lomba, J. Chem. Phys. **110**, 1148 (1999).
- ³¹ D. Beglov and B. Roux, J. Chem. Phys. **104**, 8678 (1996).
- ³² J. Richardi, P. H. Fries, and H. Krienke, J. Chem. Phys. **108**, 4079 (1998).
- ³³ D. Chandler, J. D. McCoy, and S. J. Singer, J. Chem. Phys. **85**, 5971 (1986); **85**, 5971 (1986).
- ³⁴ C. M. Cortis, P. J. Rossky, R. A. Friesner, J. Chem. Phys. **107**, 6400 (1997).
- ³⁵ D. Beglov and B. Roux, J. Phys. Chem. B **101**, 7821 (1997).
- ³⁶ A. Kovalenko and F. Hirata, Chem. Phys. Lett. **290**, 237 (1998).
- ³⁷ A. Kovalenko, S. Ten-no, and F. Hirata, J. Comput. Chem. **20**, 928 (1999).
- ³⁸ A. Kovalenko and F. Hirata, J. Phys. Chem. B **103**, 7942 (1999).
- ³⁹ A. Kovalenko and F. Hirata, J. Chem. Phys. **110**, 10095 (1999).
- ⁴⁰ A. Kovalenko and F. Hirata, J. Chem. Phys. **112**, 10391 (2000); **112**, 10403 (2000).
- ⁴¹ W. H. Press, B. P. Flannery, S. A. Teukolsky, and W. T. Vetterling, *Numerical Recipes* (Cambridge University Press, New York, 1986).
- ⁴² K. Ng, J. Chem. Phys. **61**, 2680 (1974).
- ⁴³ M. Kawata, C. M. Cortis, and R. A. Friesner, J. Chem. Phys. **108**, 4426 (1998).
- ⁴⁴ T. Morita and K. Hiroike, Prog. Theor. Phys. **23**, 1003 (1960).
- ⁴⁵ S. J. Singer and D. Chandler, Mol. Phys. **55**, 621 (1985).
- ⁴⁶ F. Garisto, P. G. Kusalik, and G. N. Patey, J. Chem. Phys. **79**, 6294 (1983).
- ⁴⁷ H.-A. Yu and M. Karplus, J. Chem. Phys. **89**, 2366 (1988).
- ⁴⁸ H.-A. Yu, B. Roux, and M. Karplus, J. Chem. Phys. **92**, 5020 (1990).
- ⁴⁹ A. Ben-Naim and Y. Marcus, J. Chem. Phys. **81**, 2016 (1984).
- ⁵⁰ D. Chandler, J. Chem. Phys. **67**, 1113 (1977).
- ⁵¹ M. P. Allen and D. J. Tildesley, *Computer Simulation of Liquids* (Oxford University Press, Oxford, 1987).
- ⁵² P. H. Hünenberger and J. A. McCammon, J. Chem. Phys. **110**, 1856 (1999).
- ⁵³ R. M. Lynden-Bell and J. C. Rasaiah, J. Chem. Phys. **107**, 1981 (1997).
- ⁵⁴ H. J. C. Berendsen, J. R. Grigera, and T. P. Straatsma, J. Phys. Chem. **91**, 6269 (1987).
- ⁵⁵ L. X. Dang, Chem. Phys. Lett. **200**, 21 (1992); J. Chem. Phys. **96**, 6970 (1992); L. X. Dang and B. C. Garrett, *ibid.* **99**, 2972 (1993); L. X. Dang, Chem. Phys. Lett. **227**, 211 (1994); D. E. Smith and L. X. Dang, J. Chem. Phys. **100**, 3757 (1994); L. X. Dang and P. A. Kollman, J. Phys. Chem. **99**, 55 (1995); L. X. Dang, J. Am. Chem. Soc. **117**, 6954 (1995).
- ⁵⁶ S. H. Lee and J. C. Rasaiah, J. Chem. Phys. **101**, 6964 (1994); J. Phys. Chem. **100**, 1420 (1996); R. M. Lynden-Bell and J. C. Rasaiah, J. Chem. Phys. **105**, 9266 (1996).
- ⁵⁷ M. Edén and M. H. Levitt, J. Magn. Reson. **132**, 220 (1998).
- ⁵⁸ E. Lomba, C. Martín, M. Lombardero, and J. A. Anta, J. Chem. Phys. **96**, 6132 (1992); M. Lombardero, C. Martín, and E. Lomba, *ibid.* **97**, 2724 (1992); C. Martín, M. Lombardero, and E. Lomba, *ibid.* **98**, 6465 (1993); M. Alvarez, E. Lomba, C. Martín, and M. Lombardero, *ibid.* **103**, 3680 (1995).
- ⁵⁹ J. A. Anta, E. Lomba, M. Alvarez, C. Martín, and M. Lombardero, J. Chem. Phys. **106**, 2712 (1997).
- ⁶⁰ F. Lado, S. M. Foiles, and N. W. Ashcroft, Phys. Rev. A **28**, 2374 (1983); F. Lado, Mol. Phys. **47**, 283 (1982); **47**, 299 (1982).
- ⁶¹ L. Verlet, Mol. Phys. **41**, 183 (1980); S. Labfik, A. Malijevský, and W. R. Smith, *ibid.* **73**, 87 (1991); **73**, 495 (1991).
- ⁶² Y. Marcus, J. Chem. Soc., Perkin Trans. 1 **82**, 233 (1986); **83**, 339 (1987); **83**, 2985 (1987).
- ⁶³ H. L. Friedman and C. V. Krishnan, *Water: A Comprehensive Treatise*, edited by F. Franks (Plenum, New York, 1973), Vol. 3.
- ⁶⁴ A. G. Sharpe, *Inorganic Chemistry*, 2nd ed. (Longman, London, 1986).
- ⁶⁵ L. X. Dang and B. M. Pettitt, J. Chem. Phys. **86**, 6560 (1987); J. Am. Chem. Soc. **109**, 5531 (1987); J. Phys. Chem. **94**, 4303 (1990).
- ⁶⁶ P. B. Balbuena, K. P. Johnston, and P. J. Rossky, J. Chem. Phys. **100**, 2706 (1996).
- ⁶⁷ J. K. Buckner and W. L. Jorgensen, J. Am. Chem. Soc. **111**, 2507 (1989).
- ⁶⁸ L. X. Dang, J. E. Rice, and P. A. Kollman, J. Chem. Phys. **93**, 7528 (1990).
- ⁶⁹ E. Guàrdia, R. Rey, and J. A. Padró, Chem. Phys. **155**, 187 (1991); J. Chem. Phys. **95**, 2823 (1991).
- ⁷⁰ P. J. Cummings and G. Stell, Mol. Phys. **44**, 529 (1981); **46**, 383 (1982).
- ⁷¹ P. J. Rossky, B. M. Pettitt, and G. Stell, Mol. Phys. **50**, 1263 (1983).
- ⁷² M. Kinoshita, Yuko Okamoto, and F. Hirata, J. Am. Chem. Soc. **120**, 1855 (1998); J. Chem. Phys. **110**, 4090 (1999).
- ⁷³ H. Kawai, T. Kikuchi, and Y. Okamoto, Protein Eng. **3**, 85 (1989); U. H. E. Hansmann and Y. Okamoto, J. Comput. Chem. **14**, 1333 (1993); M. Vasques, G. Nemethy, and H. Scheraga, Chem. Rev. **94**, 2183 (1994).
- ⁷⁴ S. R. Wilson and W. Cui, *The Protein Folding Problem and Tertiary Structure Prediction*, edited by K. M. Mertz, Jr., and S. M. Le Grand (Birkhauser, Boston, 1994), pp. 43–70.